JOC The Journal of Organic Chemistry

pubs.acs.org/joc Article

Computational Exploration of the Nature of Li$^+$-Ureide Anion Catalysis on Formation of Highly Reactive Vinyl Carbocations and Subsequent C−C Bond Forming Reactions

Woojin Lee, Hosea M. Nelson, and K. N. Houk*

Cite This: J. Org. Chem. 2023, 88, 3403−3408 Read Online

ACCESS | Metrics & More | Article Recommendations | Supporting Information

ABSTRACT: The mechanisms of the C−H insertion reactions of vinyl carbocations formed by heterolysis of vinyl trifluoromethanesulfonates (triflates) by catalytic lithiated 1,3-bis[3,5-bis(trifluoromethyl)phenyl]urea (Li$^+$-ureide) have been studied with ωB97X-D density functional theory. The ionization promoted by the Li$^+$-ureide forms a metastable intimate ion pair complex of Li$^+$-ureide-triflate anion and vinyl cation. The relative thermodynamic stabilities of isomeric alkyl cations are impacted by ion-pairing with the Li$^+$-ureide-triflate anion. We show that the C−H insertion reaction of the vinyl cation intermediate is the rate-determining step and explain the effect of the aryl substituents on the formation of the vinyl cation and its C−H insertion reactivity as well as the regioselectivity of C−H activation by the vinyl cation.

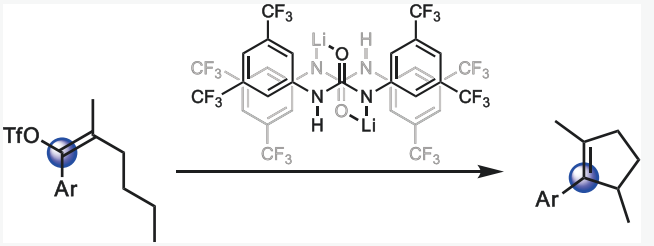

INTRODUCTION

Silylium Lewis-acid catalyzed heterolysis of vinyl triflates to form highly reactive vinyl cations, which can undergo high-yielding C−H insertion and Friedel-Crafts reactions, in nonpolar solvents were reported by Nelson, Houk, et al. in 2018.[1] Although the ionization strategy using high temperature, protic solvents, and stoichiometric acids for vinyl cation generation had been studied by Grob and Cseh,[2] Hanack,[3] Rappoport et al.,[4] and Stang et al.,[5] the formation of vinyl cations in nonpolar hydrocarbon solvents is a recent discovery.

Silylium Lewis-acid catalysts do ionize vinyl triflates, but Lewis basic heteroatoms or heterocycles interfere with the catalytic activity of silylium catalysts. In order to overcome the limitation raised by the electrophilicity of the strong Lewis acid catalyst, milder Lewis-acid lithium cations coordinated to weakly coordinating anions (WCA), such as tetrakis(pentafluorophenyl) borate were discovered.[6]

In efforts to further broaden the utility of this method, we investigated more easily accessible catalysts capable of ionizing vinyl triflates. Recently, we found Li$^+$-ureide (LiUr) catalyst **1** to be a competent Lewis acid for the heterolysis of vinyl triflates to produce vinyl cations that subsequently undergo C−C bond forming reactions (Figure 1).[7]

Vinyl carbocations are produced by the heterolysis that forms triflate coordinated to LiUr catalyst **1**. Although there have been many studies of anion-binding catalysts and their effect on the reaction mechanism of various chemical transformations,[8a−e] only a few examples have shown lithium amide catalysts as anion acceptors.[7,8f] Thus, we were unsure of the exact role of the catalyst and its influence in ion-pairing with carbocations, which prompted our computational

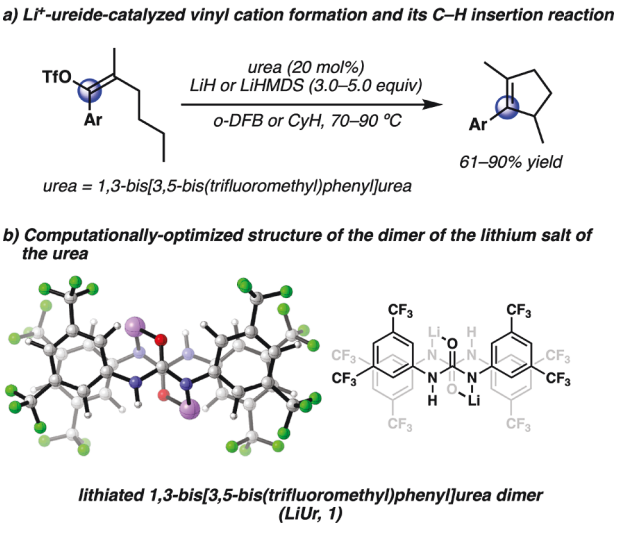

Figure 1. (a) Li$^+$-ureide-catalyzed vinyl carbocation formation and its C−C bond forming reactions. (b) Structure of the dimer of the lithium salt of the urea optimized by DFT computations.

Received: September 10, 2022
Published: February 23, 2023

https://doi.org/10.1021/acs.joc.2c02178
J. Org. Chem. 2023, 88, 3403−3408

mechanistic studies to explore the nature of Li^+-ureide catalysis and the subsequent reactivity of vinyl carbocations. Our work has shown how a complex anion interacts with a cation and the product-determining transition states, which are hypotheses previously only speculated on. We provide a detailed step-by-step vision of the role of Li^+-ureide on promoting reactions and controlling selectivities. We propose a structure of the active catalyst and show computationally how it can influence cationic reaction pathways.

COMPUTATIONAL METHODS

Density functional theory (DFT) computations were performed with Gaussian 16.[9] The ωB97X-D functional was used to optimize molecular geometries.[10] The 6-31G(d,p) basis set was employed when the number of atoms is greater than 60. Single point energies were obtained with the 6-311+G(d,p) basis set. The 6-311+G(d,p) basis set was used for optimization when the number of atoms is less than 60. A cyclohexane solvent of low dielectric constant[11] was employed in the experiment with pyridine vinyl triflate **2**.[7] Thus, geometry optimizations and single point calculations were completed in the gas phase. In order to characterize the stationary points on the potential energy surface and obtain thermal Gibbs free energy, frequency calculations were performed at the same level of theory used for geometry optimization. Gibbs free energies were corrected using GoodVibes, which corrects the vibrational frequencies *via* a quasi-harmonic approximation, as proposed by Grimme.[12] CYLview was used to visualize molecular structures.[13]

RESULTS AND DISCUSSION

While nuclear magnetic resonance spectroscopy of Li^+-ureide **1** indicated the presence of lithiate,[7] attempts at identifying a solid state structure of Li^+-ureide **1** by crystallographic means were unsuccessful. Thus, a computationally optimized (ωB97X-D/6-31G(d,p)) dimeric Li^+-ureide (LiUr) structure **1** is employed in our mechanistic studies (Figure 1b). Aggregation of lithium amides is well known, and we adopted this dimer as a simple model of potential catalytic aggregates.[14,15]

The proposed catalytic cycle is shown in Figure 2. The mechanism involves the formation of active Li^+-ureide catalyst **1**, which catalyzes heterolysis of vinyl triflate **2** to form vinyl cation **3**, insertion of cation into a C−H bond, and deprotonation of tertiary cation **4** to produce **5**.

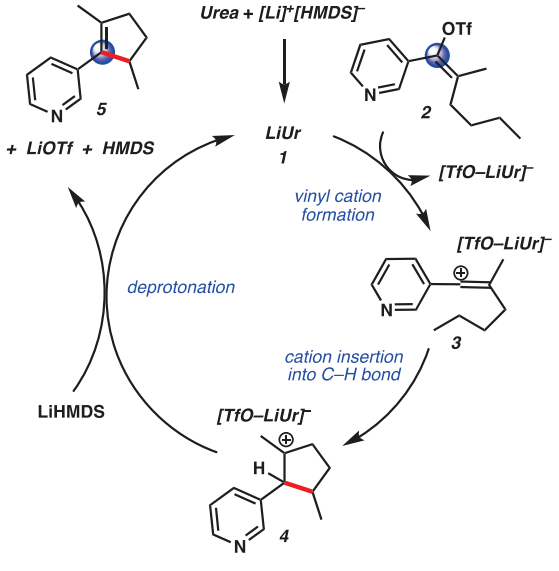

Figure 2. Proposed reaction mechanism.

We computationally explored the overall reaction mechanism with LiUr catalyst **1** and pyridine vinyl triflate **2**, which gives product **5** in 80% yield. Gibbs free energies (in kcal/mol) are obtained at 298.15 K, and the energetics are summarized in Figure 3, assuming the dimeric lithium ureide is the catalyst. The coordination of LiUr catalyst **1** to vinyl triflate substrate **6** leads to a complex **7**. This coordination is computed to be favorable by 14.4 kcal/mol. Cleavage of the C−O bond gives ion-pairing complex **9** (−1.0 kcal/mol), with TS **8** at 1.3 kcal/mol. There is a negligible barrier for the reversible formation of complex **7** from ion-pairing complex **9**. As shown in Figure 4, a contact of 3.06 Å between Li^+-ureide-triflate anion and vinyl cation is observed in ion-pairing complex **9**. An intimate ion pair, which was originally introduced by Winstein et al., is seen in this structure.[16] A concerted C−H insertion occurs *via* TS **10** at 5.9 kcal/mol to form **11** (−28.2 kcal/mol). The C−H insertion step is the rate-determining step.[17] The transition state **10** computed for this reaction is shown in Figure 4. Note that the transition state is essentially a hydride abstraction, but the generation of the alkene with its π bond directly interacting with the secondary cation vacant orbital leads to the insertion product **11** with no additional barrier. This is a two-stage concerted process. Finally, a highly exergonic deprotonation by excess LiHMDS forms product **5**.

We find that the hydride shift from **11** to **13** is thermodynamically unfavorable in the ion pair even though **13** is a benzylic carbocation. As shown in Figure 4, distances from oxygens that consist of negatively charged ions to a positively charged carbon atom in complex **11** are 3.72 and 2.93 Å. On the other hand, in complex **13**, distances between anionic oxygens and a cationic carbon are 4.16 and 4.93 Å. Structural analysis exhibits that the ion-pair interactions are stronger in complex **11**. Calculations on these reactions in the absence of a counter anion show that pyridine benzylic cation **20c** is more stable than tertiary cation **18c** by 2.5 kcal/mol (Figure 5a). The relative stabilities of the tri-coordinated carbocations are changed by the effect of ion pairing. Thus, we propose that the deprotonation step occurs directly from **11**.

Computational model substrates (Ar = *p*-anisyl and phenyl) were employed to evaluate the electronic effects in the C−H insertion reaction (Figure 5a, Gibbs free energies in kcal/mol). Triflate affinity energies, which measure the energy to generate the vinyl cation from the triflate, are utilized as a reference to compare the energetics of the ions.[18] As shown in Figure 5a, vinyl cation **16** undergoes the concerted C−H insertion reaction *via* TS **17** to generate tertiary carbocation **18**, which is followed by 1,2-hydride shift through TS **19** in order to form benzylic cation **20**. IRC calculations of TS **17** predicted the concerted C−H insertion pathway. The activation energy barriers of the C−H insertion reactions are affected by the stability of vinyl cation intermediates. With the relatively electron-withdrawing pyridyl group, the vinyl cation intermediate is less stabilized than by phenyl or anisyl. The activation energy barrier for the C−H insertion reaction is the lowest with pyridyl and higher with phenyl and anisyl (Figure 5a).

The regioselectivity in C−H activation by the vinyl carbocation was also studied (Figure 5b). The two-stage concerted process (**17d**, 11.5 kcal/mol) forms 6-membered ring **18d**. The process generates the primary cation vacant orbital through the 1,6-hydride abstraction in the first stage.

https://doi.org/10.1021/acs.joc.2c02178
J. Org. Chem. 2023, 88, 3403−3408

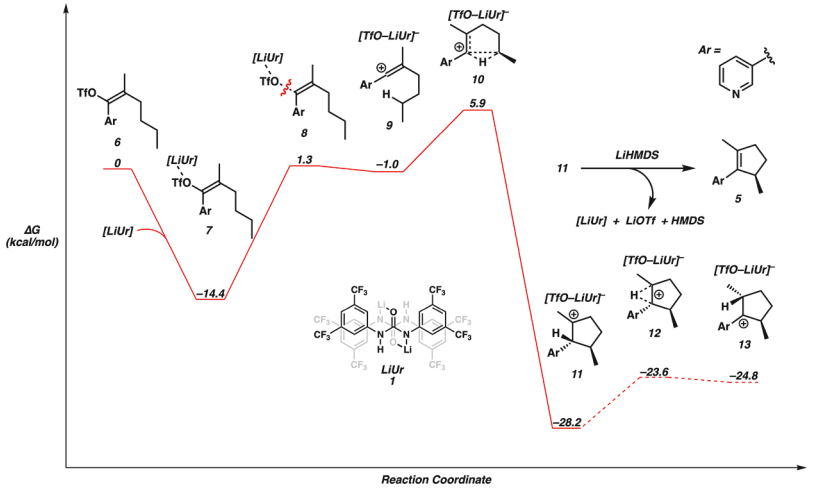

Figure 3. Computational investigation of the overall reaction process with ωB97X-D/6-311+G(d,p) // ωB97X-D/6-31G(d,p) in the gas phase at 298.15 K.

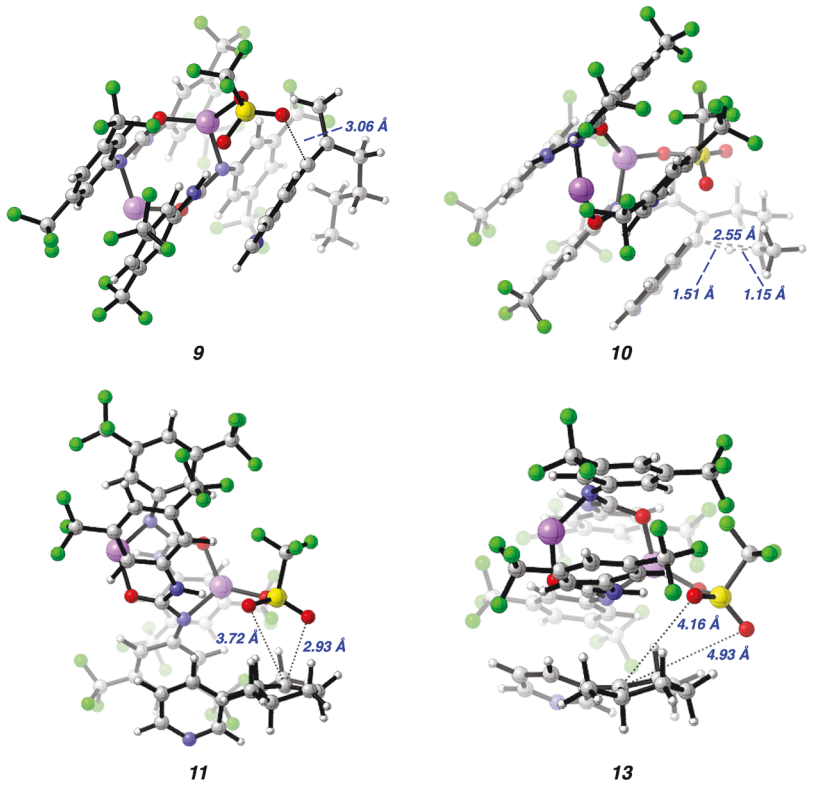

Figure 4. 3D structures of complexes **9**, **11**, and **13** and C−H insertion transition state **10**.

The generation of the primary cation is more difficult than the generation of the secondary cation, which is observed in **17c** in the formation of 5-membered ring **18c**. The reaction is possible, but the competing reaction pathway **17c** (4.2 kcal/mol) is kinetically favored. Moreover, we attempted computational location of the transition state for formation of the 4-membered ring, but the computational studies predict formation of the bridged cation **18e** *via* concerted 1,4-hydride abstraction **17e** (13.0 kcal/mol). This hypothetical pathway is less favorable than the formation of **17c**.

CONCLUSIONS

We have investigated the mechanism of a vinyl carbocation C−H insertion reaction with a dimeric Li^+-ureide catalyst. We show that the catalyst not only generates vinyl carbocations from vinyl triflates, but also forms an ion pair of the cation with Li^+-ureide triflate anion rather than the ureide anion proposed before.[7] Because of the reversible nature of the catalyzed heterolysis, the subsequent C−H insertion step can be the rate-determining step. In previous work, the heterolysis is rate-determining, because ionization of 1-cyclohexenyl triflate is slow due to the nonlinear geometry forced on the cyclohexenyl *sp*-hybridized cation.[1,17] By contrast, the ionization of substrates that can form aryl-substituted linear vinyl cations

https://doi.org/10.1021/acs.joc.2c02178
J. Org. Chem. 2023, 88, 3403−3408

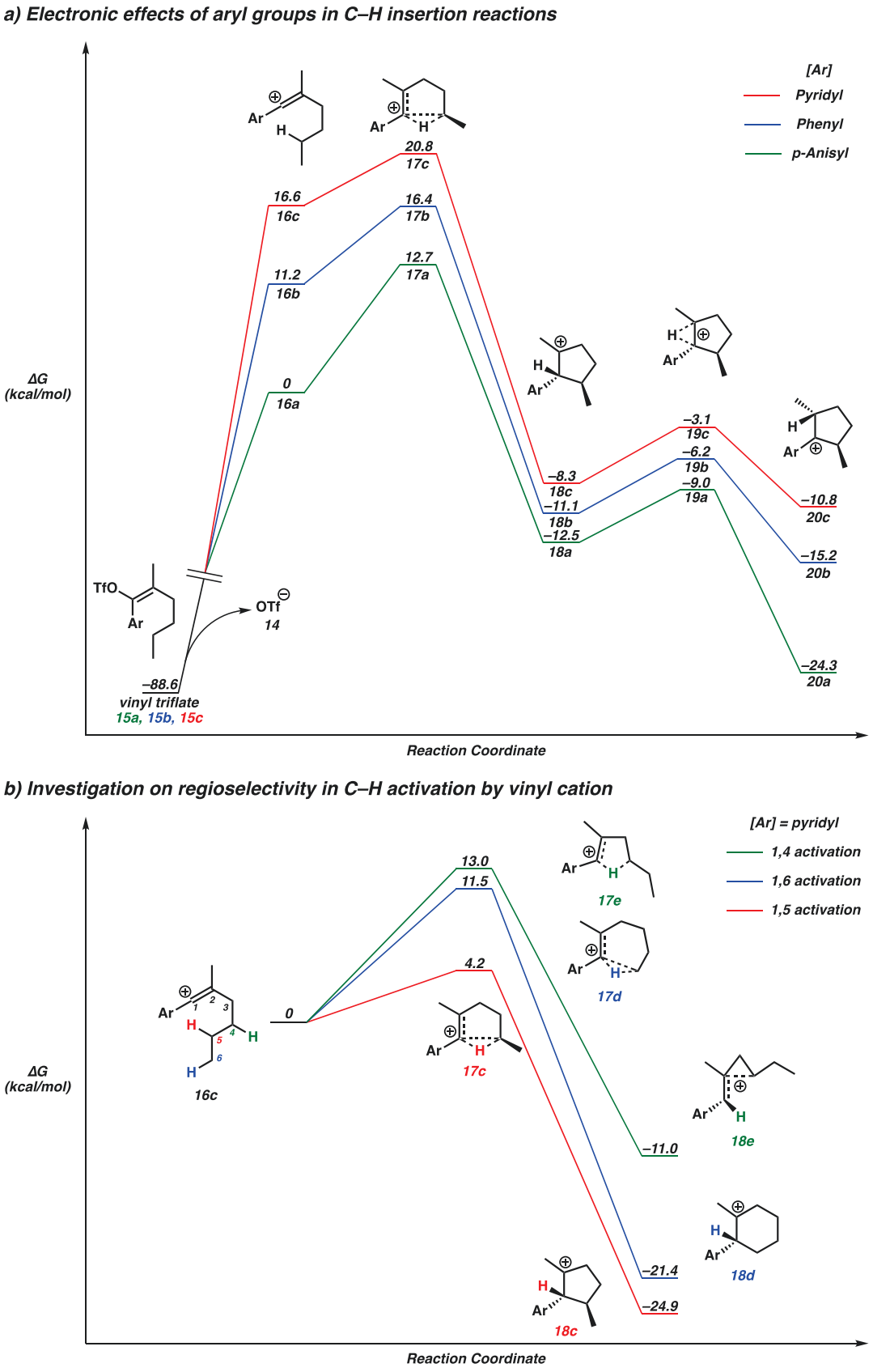

Figure 5. Computational studies of the vinyl cation reactivity in the absence of counter anion with ωB97X-D/6-311+G(d,p) in the gas phase at 298.15 K.

is easier, and the rate of C−H insertion can be influenced by aryl substituents. The reactivity difference of anisyl, phenyl, and pyridyl vinyl cations in C−H insertion reactions has been measured theoretically in this work. We have also explained

https://doi.org/10.1021/acs.joc.2c02178
J. Org. Chem. 2023, 88, 3403−3408

why the formation of the five-membered ring product through the C−H insertion reaction is favored over four- and six-membered ring formation.[7]

Finally, during the revision of this manuscript, our groups have described an enantioselective vinyl cation C−H insertion reaction.[19] Our studies of vinyl carbocations generated from the Li^+-ureide catalyst provide further evidence for the nature of ion pairs generated in these reactions.

■ ASSOCIATED CONTENT

Data Availability Statement

The data underlying this study are available in the published article and its Supporting Information.

Supporting Information

The Supporting Information is available free of charge at https://pubs.acs.org/doi/10.1021/acs.joc.2c02178.

Energies and Cartesian coordinates of all optimized structures and transition state structures (PDF)

■ AUTHOR INFORMATION

Corresponding Author

K. N. Houk − *Department of Chemistry and Biochemistry, University of California, Los Angeles, California 90095, United States;* orcid.org/0000-0002-8387-5261; Email: houk@chem.ucla.edu

Authors

Woojin Lee − *Department of Chemistry and Biochemistry, University of California, Los Angeles, California 90095, United States;* orcid.org/0000-0002-8531-0301

Hosea M. Nelson − *Division of Chemistry and Chemical Engineering, California Institute of Technology, Pasadena, California 91125, United States*

Complete contact information is available at: https://pubs.acs.org/10.1021/acs.joc.2c02178

Author Contributions

The manuscript was written through contributions of all authors. All authors have given approval to the final version of the manuscript.

Notes

The authors declare no competing financial interest.

■ ACKNOWLEDGMENTS

Financial support of this work was generously provided by the National Science Foundation (CHE-1764328 to K.N.H.). W.L. is grateful for additional funding from the UCLA Graduate Dean's Scholar Award. We thank Stasik Popov and Benjamin Wigman for the discussions of the experimental results. Computations were performed on the UCLA Institute of Digital Research and Education Hoffman2 Cluster.

■ REFERENCES

(1) Popov, S.; Shao, B.; Bagdasarian, A. L.; Benton, T. R.; Zou, L.; Yang, Z.; Houk, K. N.; Nelson, H. M. Teaching an old carbocation new tricks: intermolecular C−H insertion reactions of vinyl cations. *Science* **2018**, *361*, 381−387.

(2) Grob, C. A.; Cseh, G. Die Solvolyse von α-Bromstyrolen Substitution am ungesättigten trigonalen Kohlenstoffatom. *Helv. Chim. Acta* **1964**, *47*, 194−203.

(3) (a) Hanack, M. Vinyl Cations in Solvolysis Reactions. *Acc. Chem. Res.* **1970**, *3*, 209−216. (b) Hanack, M. Stabilized Vinyl Cations. *Acc. Chem. Res.* **1976**, *9*, 364−371. (c) Hanack, M. Mechanistic and Preparative Aspects of Vinyl Cation Chemistry. *Angew. Chem., Int. Ed. Engl.* **1978**, *17*, 333−341.

(4) (a) Rappoport, Z.; Gal, A. Vinylic Cations from Solvolysis. I. Trianisylvinyl halide system. *J. Am. Chem. Soc.* **1969**, *91*, 5246−5254. (b) Rappoport, Z.; Apeloig, Y. Vinylic cations from solvolysis. II. Stereochemistry of the SN1 reaction of 1,2-dianisyl-2-phenylvinyl halides. *J. Am. Chem. Soc.* **1969**, *91*, 6734−6742. (c) Rappoport, Z.; Kaspi, J. Vinylic cations from solvolysis. III. Solvolysis of triarylvinyl arylsulfonates in aqueous acetone. *J. Am. Chem. Soc.* **1970**, *92*, 3220−3221. (d) Rappoport, Z.; Kaspi, J. Vinylic cations from solvolysis. XVIII. Unusual solvent effects and external ion return in the solvolysis of several vinylic compounds in aqueous trifluoroethanol. *J. Am. Chem. Soc.* **1974**, *96*, 4518−4530.

(5) (a) *Vinyl Cations*; Stang, P.; Rappoport, Z.; Hanack, M.; Subramanian, L. R., Eds.; Academic Press: New York, 1979. (b) *Dicoordinated Cations*; Rappoport, Z.; Stang, P. J., Eds.; Wiley: New York, 1997. (c) Stang, P. J.; Summerville, R. Preparation and solvolysis of vinyl trifluoromethanesulfonates. I. evidence for simple alkylvinyl cation intermediates. *J. Am. Chem. Soc.* **1969**, *91*, 4600−4601. (d) Stang, P. J.; Anderson, A. G. Preparation and chemistry of vinyl triflates. 16. mechanism of alkylation of aromatic substrates. *J. Am. Chem. Soc.* **1978**, *100*, 1520−1525.

(6) Wigman, B.; Popov, S.; Bagdasarian, A. L.; Shao, B.; Benton, T. R.; Williams, C. G.; Fisher, S. P.; Lavallo, V.; Houk, K. N.; Nelson, H. M. Vinyl carbocations generated under basic conditions and their intramolecular C−H insertion reactions. *J. Am. Chem. Soc.* **2019**, *141*, 9140−9144.

(7) (a) Bagdasarian, A. L.; Popov, S.; Wigman, B.; Wei, W.; Lee, W.; Nelson, H. M. Urea-catalyzed vinyl carbocation formation enables mild functionalization of unactivated C−H bonds. *Org. Lett.* **2020**, *22*, 7775−7779. (b) We use the generic term of "ureide" to refer to the anion formed by deprotonation of 1,3-bis[3,5-bis(trifluoromethyl) phenyl]urea.

(8) (a) Seidel, D. The Anion-Binding Approach to Catalytic Enantioselective Acyl Transfer. *Synlett* **2014**, *25*, 783−794. (b) Zhang, Z.; Schreiner, P. R. (Thio)urea organocatalysis−What can be learnt from anion recognition? *Chem. Soc. Rev.* **2009**, *38*, 1187−1198. (c) Beckendorf, S.; Asmus, S.; García Mancheño, O. H-Donor Anion Acceptor Organocatalysis−The Ionic Electrophile Activation Approach. *ChemCatChem* **2012**, *4*, 926−936. (d) Brak, K.; Jacobsen, E. N. Asymmetric Ion-Pairing Catalysis. *Angew. Chem., Int. Ed.* **2013**, *52*, 534−561. (e) Visco, M. D.; Attard, J.; Guan, Y.; Mattson, A. E. Anion-binding catalyst designs for enantioselective synthesis. *Tetrahedron Lett.* **2017**, *58*, 2623−2628. (f) Sharma, H. A.; Essman, J. Z.; Jacobsen, E. N. Enantioselective catalytic 1,2-boronate rearrangements. *Science* **2021**, *374*, 752−757.

(9) Frisch, M. J.; Trucks, G. W.; Schlegel, H. B.; Scuseria, G. E.; Robb, M. A.; Cheeseman, J. R.; Scalmani, G.; Barone, V.; Petersson, G. A.; Nakatsuji, H.; Li, X.; Caricato, M.; Marenich, A. V.; Bloino, J.; Janesko, B. G.; Gomperts, R.; Mennucci, B.; Hratchian, H. P.; Ortiz, J. V.; Izmaylov, A. F.; Sonnenberg, J. L.; Williams-Young, D.; Ding, F.; Lipparini, F.; Egidi, F.; Goings, J.; Peng, B.; Petrone, A.; Henderson, T.; Ranasinghe, D.; Zakrzewski, V. G.; Gao, J.; Rega, N.; Zheng, G.; Liang, W.; Hada, M.; Ehara, M.; Toyota, K.; Fukuda, R.; Hasegawa, J.; Ishida, M.; Nakajima, T.; Honda, Y.; Kitao, O.; Nakai, H.; Vreven, T.; Throssell, K.; Montgomery, J. A., Jr.; Peralta, J. E.; Ogliaro, F.; Bearpark, M. J.; Heyd, J. J.; Brothers, E. N.; Kudin, K. N.; Staroverov, V. N.; Keith, T. A.; Kobfayashi, R.; Normand, J.; Raghavachari, K.; Rendell, A. P.; Burant, J. C.; Iyengar, S. S.; Tomasi, J.; Cossi, M.; Millam, J. M.; Klene, M.; Adamo, C.; Cammi, R.; Ochterski, J. W.; Martin, R. L.; Morokuma, K.; Farkas, O.; Foresman, J. B.; Fox, D. J. *Gaussian 16*; Gaussian, Inc.: Wallingford, CT, 2016.

(10) Chai, J.-D.; Head-Gordon, M. Long-range corrected hybrid density functionals with damped atom−atom dispersion corrections†. *Phys. Chem. Chem. Phys.* **2008**, *10*, 6615−6620.

(11) Richards, T. W.; Shipley, J. W. The dielectric constants of typical alphatic and aromatic hydrocarbons, cyclohexane, cyclohexanone, and cyclohexanol. *J. Am. Chem. Soc.* **1919**, *41*, 2002−2012.

(12) (a) Grimme, S. Supramolecular binding thermodynamics by dispersion-corrected density functional theory. *Chem. – Eur. J.* **2012**, *18*, 9955–9964. (b) Luchini, G.; Alegre-Requena, J. V.; Guan, Y.; Funes-Ardoiz, I.; Paton, R. S. *GoodVibes: GoodVibes 3.0.1*; 2019. DOI: 10.5281/zenodo.595246.
(13) Legault, C. Y. *CYLview, 1.0b*; Universite′ de Sherbrooke, 2009; http://www.cylview.org.
(14) (a) Reich, H. J. Role of organolithium aggregates and mixed aggregates in organolithium mechanisms. *Chem. Rev.* **2013**, *113*, 7130–7178. (b) Harrison-Marchand, A.; Mongin, F. Mixed aggregate (MAA): a single concept for all dipolar organometallic aggregates. 1. structural data. *Chem. Rev.* **2013**, *113*, 7470–7562.
(15) Williard, P. G.; Salvino, J. M. Synthesis, isolation, and structure of an LDA-THF complex. *J. Org. Chem.* **1993**, *58*, 1–3.
(16) Winstein, S.; Clippinger, E.; Fainberg, A. H.; Heck, R.; Robinson, G. C. Salt effects and ion pairs in solvolysis and related reactions. III.[1] common ion rate depression and exchange of anions during acetolysis[2,3]. *J. Am. Chem. Soc.* **1956**, *78*, 328–335.
(17) The measurement of k_H/k_D of the C–H insertion reaction of a cyclohexenyl vinyl triflate with cyclohexane and cyclohexane-d_{12} is 0.96, implying that formation of the strained cyclohexenyl vinyl cation is rate-determining.[1] By contrast, in the example in Figure 3, the cation will be formed more readily and the C–H insertion reaction will be slower. We expect a normal kinetic isotope effect.
(18) See the Supporting Information for details (Figure S5)
(19) Nistanaki, S. K.; Williams, C. G.; Wigman, B.; Wong, J. J.; Haas, B. C.; Popov, S.; Werth, J.; Sigman, M. S.; Houk, K. N.; Nelson, H. M. Catalytic asymmetric C–H insertion reactions of vinyl carbocations. *Science* **2022**, *378*, 1085–1091.

https://doi.org/10.1021/acs.joc.2c02178
J. Org. Chem. 2023, 88, 3403–3408